Supplementary Information for 'A physical model of the high-frequency seismic signal generated by debris flows'

Maxime Farin[1], Victor C. Tsai[1], Michael P. Lamb[1] and Kate Allstadt[2]

1. Division of Geological and Planetary Sciences, California Institute of Technology. Pasadena, CA 91125, USA
2. USGS Geological Hazards Science Center. Golden CO, USA

November 19, 2018

Contents

1 High Frequencies Generated by Flow Motion Around Obstacles

Here, we evaluate the conditions for which fluctuations in static stresses caused by large scale interactions generate high-frequency signals. If a section of a debris flow is flowing down a slope with an imposed downslope speed, u_x, variations in the basal topography affects the static stresses the flow applies on the bed by introducing a normal fluctuating bulk acceleration.

We consider a cosine slope $L\cos 2\pi x/\lambda$, with λ the slope wavelength and L, the amplitude of the obstacles (Fig. S1). The normal bulk acceleration of the flow section is $a_z(t) = L\omega^2\cos\omega t$, where t is time and $\omega = 2\pi u_x/\lambda$ is the circular frequency. a_z then fluctuates between peaks $-L\omega^2$ and $L\omega^2$ at characteristic frequency $f = \omega/2\pi = u_x/\lambda$.

Therefore, fluctuations in the flow normal acceleration can generate large high-frequency (> 1 Hz) fluctuations in basal stresses if the flow speed, u_x, is large enough and if the characteristic wavelength, λ, of the bed topography, i.e. the size of the obstacles, is small enough (Fig. S1). For example, if we

assume $L = \lambda/2$ and $u_x = 1$ m s^{-1}, the characteristic frequency is above 1 Hz when the flow moves around obstacles of size smaller than $\lambda \approx 0.5$ m while for $u_x = 10$ m s^{-1}, generated frequencies are $f \sim 10 - 50$ Hz for obstacles smaller than $\lambda \approx 2$ m.

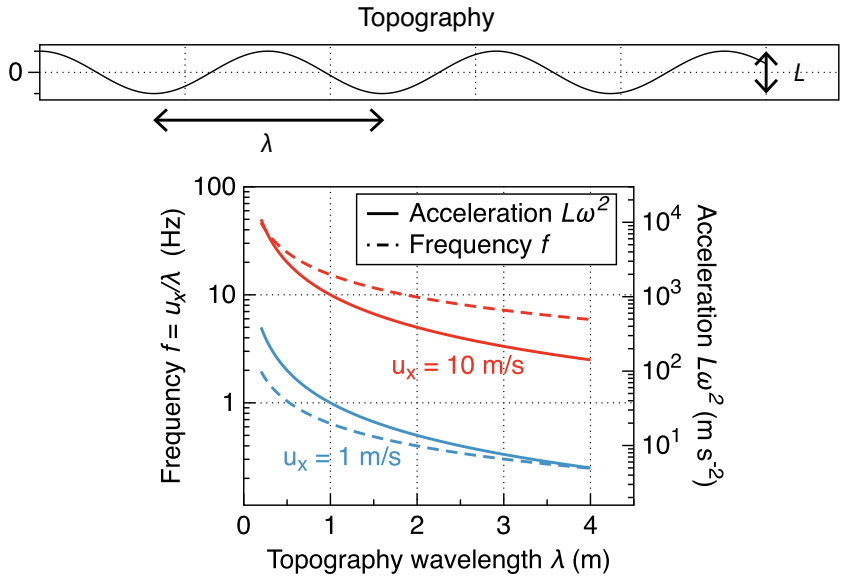

Figure S1: Normal peak acceleration $L\omega^2$ and frequency $f = u_x/\lambda$ of variation of the acceleration of a section of the debris flow moving with imposed downslope speed u_x down a cosine slope $L\cos 2\pi x/\lambda$, with λ and L the topography wavelength and amplitude, for $u_x = 1$ m s^{-1} and $u_x = 10$ m s^{-1}, as functions of λ. We assume here that the amplitude L of the obstacles is $L = \lambda/2$.

2 Influence of Bed Roughness on the Basal Impulses

The bed roughness affects the angle α (between the direction of impact impulse and the normal to the bed) and, therefore, the characteristic basal impulse (RMS of the basal impulses for all possible values of α, see Appendix A of the main manuscript). For a flat bed, the impact impulse is normal to the bed (tangential impulse is zero) and $\alpha = 0$ (Fig. S2a and S2c). Typical bed roughness can be modeled by successive bumps of diameter D_b separated by average distance ϵ (Fig. S2bc). With this roughness, the maximum value of the angle α, α_m, depends on the value of ϵ compared with the particle diameter D. When $\epsilon < D_b(\sqrt{1 + 2D/D_b} - 1)$, $\alpha_m = \arcsin(\frac{\epsilon + D_b}{D + D_b})$ (Fig. S2b) and when $\epsilon > D_b(\sqrt{1 + 2D/D_b} - 1)$ then $\alpha_m = \arccos(\frac{D}{D + D_b})$ (Fig. S2c). When the

particle diameter, D, is small compared to the roughness dimension, D_b, f_z is smaller than on a flat bed and f_x is larger than on a flat bed (Fig. S2d), with asymptotes to the flat-bed case as $D/D_b \to \infty$, since $\alpha_m \to 0$. The convergence is slower as ϵ/D_b increases. For a flat bed, the integrals defined in Eq. (A.5) of the main text can be performed analytically to solve for f_z, with the result being $f_z = 1/\sqrt{3} \cdot \delta u/u_x$. Thus, for the case $\delta u/u_x = 1$ shown in Fig. S2d, $f_z = 1/\sqrt{3} \approx 0.577$ (see solid red line in Fig. S2d). In the flat bed case, $f_x = f_y = 0$ (see dashed red line in Fig. S2d).

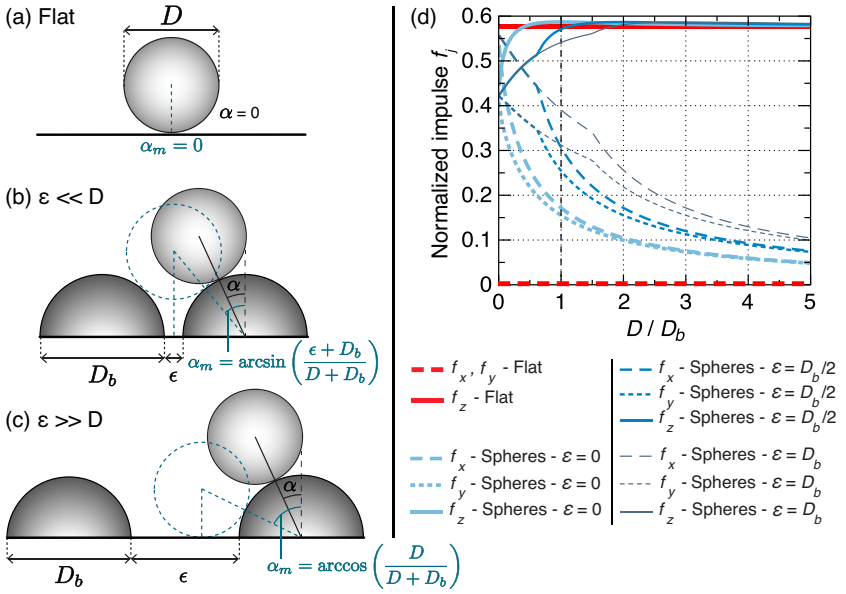

Figure S2: (a), (b) and (c) Schematic for beds with different geometries: (a) Flat bed and (b,c) rough beds made of fixed spheres of diameter D_b, separated by distance ϵ. The maximum value of α, α_m, depends on the value of ϵ. (d) Normalized impulses $f_j = \bar{I}_j/((1+e_b)mu_x)$ as in Fig. 3 of the main text, for the case $\delta u = u_x$, as a function of D/D_b and for various values of ϵ. The solid red line describes $f_z = 1/\sqrt{3}$ in the flat bed case and the dashed red line describes $f_x = f_y = 0$ in the flat bed case. Results for f_j asymptote to the flat bed results as $D/D_b \to \infty$.

3 Exact and Approximate Fluctuating Speeds in Thick Debris Flows Derived from the Kinetic Theory of Dense Granular Gases

Energy Equation and Approximate Solution

For debris flows in the thick-flow limit ($D/h \ll 1$), we evaluated the average basal fluctuating speed due to interactions with the bed roughness to be

$$\delta u_{rough} \approx \frac{(p+1)D\overline{u}_x}{2h}, \tag{S1}$$

where $\overline{u}_x$ is depth-averaged flow speed, D is particle diameter, h is flow thickness and $p \geq 1$ is the power of the flow profile $u_x(z) = C(h^p - (h-z)^p)$, with C a constant.

An alternative estimate of the average basal fluctuating speed δu in the thick-flow limit can be made by using the kinetic theory of dense granular gases (see e.g. *Hutter*, 1993; *Rao and Nott*, 2008; *Andreotti et al.*, 2013). Within this formalism, we aim to determine the average fluctuating speed as a function of height within the flow, $\delta u(z)_{kin}$, and the average basal fluctuating speed is then given by $\delta u(0)_{kin}$. For steady, uniform flows, the granular temperature $T = \delta u_{kin}^2$ is the result of competition between production of particle agitation due to the work of shear stress τ_{xz} through the speed gradient $\frac{\mathrm{d}u_x}{\mathrm{d}z}$ and dissipation of agitation due to inelastic collisions between particles. At locations where production and dissipation of particle agitation do not balance, particle agitation is assumed to be transported from or to neighboring areas with the flux $q_z = -K\frac{\mathrm{d}T}{\mathrm{d}z}$, where K is analogous to thermal conductivity. The governing equation for granular temperature T is then (e.g. *Jenkins and Askari*, 1999; *Rao and Nott*, 2008; *Lee and Huang*, 2012; *Andreotti et al.*, 2013)

$$\frac{\mathrm{d}}{\mathrm{d}z}\left(K\frac{\mathrm{d}T}{\mathrm{d}z}\right) + \tau_{xz}\frac{\mathrm{d}u_x}{\mathrm{d}z} - \Gamma = 0. \tag{S2}$$

where $-\Gamma$ represents the inelastic loss of power per unit volume. The solid static shear stress is given by $\tau_{xz}(z) = (\rho_s - \rho_f)\phi g \sin\theta(h-z)$ with ρ_s and ρ_f, the density of the particles and of the interstitial fluid, respectively, ϕ, the particle fraction, g, the gravitational acceleration and θ, the slope angle (*Iverson*, 1997).

In order to solve Eq. (S2) for the average fluctuating speed $\delta u(z)_{kin} = \sqrt{T(z)}$, we need to express K and Γ as functions of $T(z)$ or z. Simple expressions for K and Γ with undetermined multiplicative constants K' and Γ' can be obtained with physical intuition and scaling arguments (e.g. *Haff*, 1983; *Rao and Nott*, 2008; *Andreotti et al.*, 2013). Since $K \sim q_z/\frac{dT}{dz}$, it can be estimated as

$$K \sim \frac{\text{energy per collision} \cdot \text{collision rate}}{\text{surface area} \cdot \frac{dT}{dz}} \sim \frac{\rho_s D^3 \delta u_{kin}^2 \cdot \frac{\delta u_{kin}}{s}}{D^2 \cdot \delta u_{kin}^2 / D} \sim \rho_s D^2 \delta u_{kin}/s, \tag{S3}$$

where s is the characteristic distance between impact events, which is set by the inter-particle distance. Similarly, Γ can be estimated as

$$\Gamma \sim \frac{\text{energy lost per col.} \cdot \text{col. rate}}{\text{volume}} \sim \frac{(1-e^2)\rho_s D^3 \delta u_{kin}^2 \cdot \frac{\delta u_{kin}}{s}}{D^3} \sim (1-e^2)\rho_s \delta u_{kin}^3/s, \tag{S4}$$

where e is the coefficient of restitution of the particles within the flow. In the following, we assume that the scaling estimates of Eqs. (S3)-(S4) are accurate, such that $K = \rho_s D^2 \delta u_{kin}/s$ and $\Gamma = (1-e^2)\rho_s \delta u_{kin}^3/s$, i.e. that multiplicative constants K' and Γ' that could have multiplied these expressions are equal to 1. For this model, s is the average closest distance between particles, which can be related to the particle fraction ϕ by noting that a particle occupies a volume $\sim (D+s)^3$, and it would occupy a volume $\sim D^3$ at the maximum bulk particle fraction ϕ_{max}. Therefore, for small s,

$$\frac{\phi}{\phi_{max}} \approx \left(\frac{D}{D+s}\right)^3. \tag{S5}$$

and

$$s \approx D\left(\left(\frac{\phi_{max}}{\phi}\right)^{1/3} - 1\right). \tag{S6}$$

Uncertainties in the basal average fluctuating speed $\delta u(0)_{kin}$ due to the assumption that $K' = \Gamma' = 1$ are less than 20% compared to cases where more realistic values of the constants are used ($K' \sim 0.3 - 0.9$ and $\Gamma' \sim 0.7 - 1.4$ (e.g. *Lun et al.*, 1984; *Jenkins and Askari*, 1999)).

Substituting for τ_{xz}, $\frac{\mathrm{d}u_x}{\mathrm{d}z}$ (with $u_x(z)$ as defined above), K and Γ into Eq. (S2), we obtain the simplified energy equation (e.g. *Lee and Huang*, 2012)

$$\frac{\mathrm{d}^2 T^{3/2}}{\mathrm{d}z^2} = AT^{3/2} - B(p+1)\overline{u}_x(1-z/h)^p, \tag{S7}$$

$$A = \frac{3(1-e^2)}{2D^2}, \tag{S8}$$

$$B = \frac{3s\phi g' \sin\theta}{2D^2}, \tag{S9}$$

where the depth-averaged flow speed is $\overline{u}_x = Cph^p/(p+1)$.

Equation (S7) has a solution and can be solved analytically with specific boundary conditions, which are uncertain. Before determining this exact solution (see next section), we observe that Eq. (S7) has an approximate solution that can be obtained by balancing local dissipation and production, and ignoring the $\frac{\mathrm{d}^2 T^{3/2}}{\mathrm{d}z^2}$ transport term on the left hand side of Eq. (S7). This balance results in

$$T(z) \approx \left(\frac{B}{A}(p+1)\overline{u}_x(1-z/h)^p\right)^{2/3}. \tag{S10}$$

Substituting Eqs. (S8) and (S9) for A and B then results in

$$\delta u(0)_{kin} = \sqrt{T(0)} \approx \left(\frac{s\phi g' \sin\theta}{1-e^2}(p+1)\overline{u}_x\right)^{1/3}. \tag{S11}$$

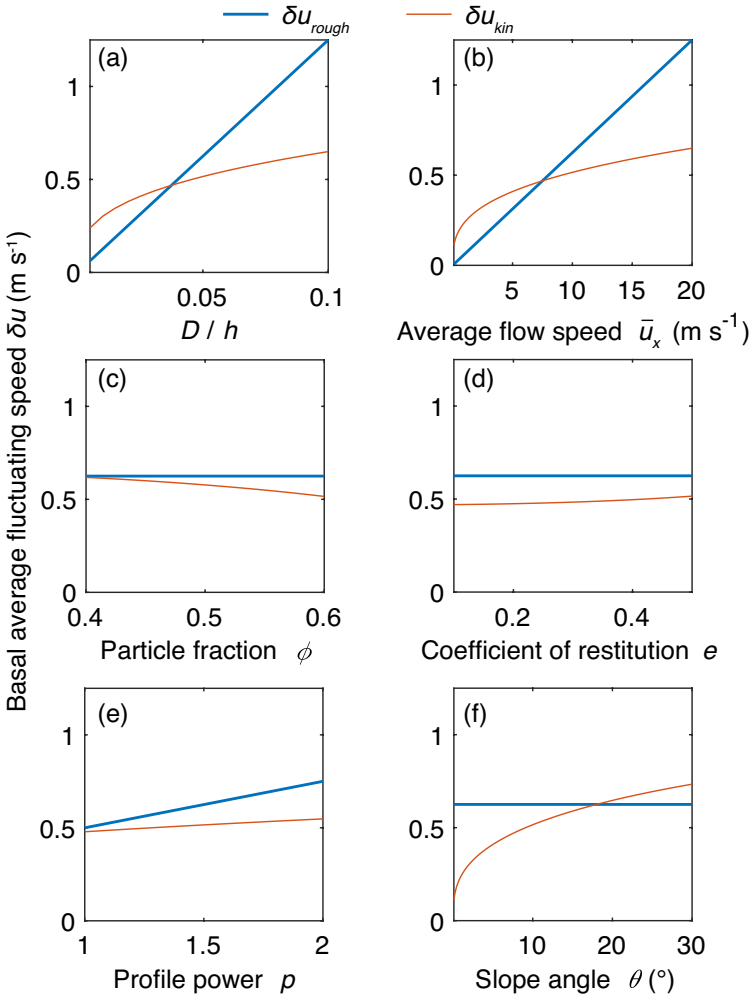

Figure S3: Comparison of δu_{rough} (Eq. (S1)) and $\delta u(0)_{kin}$ (Eq. (S11)) as a function of (a) D/h, (b) $\overline{u}_x$, (c) ϕ, (d) e, (e) p and (f) θ. When not varied, flow parameters are set as $D = 0.1$ m, $h = 2$ m, $\overline{u}_x = 10$ m s^{-1}, $\phi = 0.6$, $e = 0.5$, $p = 3/2$ and $\theta = 10°$. Other flow parameters are $\rho_s = 2500$ kg m^{-3}, $\rho_f = 1500$ kg m^{-3} and $\phi_{max} = 0.8$.

We compare $\delta u(0)_{kin}$ predicted by the kinetic theory of Eq. (S11) with δu_{rough} predicted by Eq. (S1) as various flow parameters are varied. The main difference is that Eq. (S1) depends linearly on D and $\overline{u}_x$ whereas Eq. (S11) depends on D and $\overline{u}_x$ to the 1/3 power (see also Fig. S3). δu_{rough} therefore dominates over $\delta u(0)_{kin}$ for larger ratios D/h and for larger flow speeds $\overline{u}_x$. ϕ, e and p have little influence on δu within realistic ranges of those parameters

(Fig. S3cde). The influence of slope angle, θ, on $\delta u(0)_{kin}$ may be stronger than shown in Fig. S3f because θ also affects $\overline{u}_x$, which is fixed in this plot.

Exact Solution and Boundary Conditions

Exact Solution

Here we solve the energy equation, Eq. (S7), for the specific case of a Bagnold speed profile ($p = 3/2$). We can write the energy equation in the form

$$\frac{\mathrm{d}^2 S(z)}{\mathrm{d}z^2} = AS(z) - \frac{3BC}{2}(h-z)^{3/2}, \tag{S12}$$

with $S = T^{3/2}$ and A and B given by equations (S8) and (S9), and C can again be rewritten in terms of $\overline{u}_x$ as above, with $p = 3/2$, as $C = 5\overline{u}_x/(3h^{3/2})$.

The analytical solution of Eq. (S12) is

$$\begin{aligned} S(z) = T^{3/2}(z) \quad = \quad & -\frac{9\sqrt{\pi}BC}{16A^{7/4}}[\mathrm{erf}(A^{1/4}\sqrt{h-z})\exp(\sqrt{A}(h-z)) \\ & -\mathrm{erfi}(A^{1/4}\sqrt{h-z})\exp(-\sqrt{A}(h-z))] \\ & +\frac{3BC}{2A}(h-z)^{3/2} + c_1\exp(\sqrt{A}z) + c_2\exp(-\sqrt{A}z), \end{aligned} \tag{S13}$$

where erf() and erfi() are the error function and the imaginary error function and c_1 and c_2 are two constants to determine from the boundary conditions.

Boundary Conditions

There is no shear stress and therefore no production of granular temperature at the free surface. We may then take $T(z = h) = 0$. This first boundary condition leads to

$$c_1\exp(\sqrt{A}h) + c_2\exp(-\sqrt{A}h) = 0 \tag{S14}$$

The second boundary condition is expressed at the bed. Some authors (e.g. *Lee and Huang*, 2012) assume that the granular temperature is zero at the bed, which is the simplest way to solve the equation but it means that the bed completely dissipates granular agitation. However, bumps in the basal roughness can provide a normal speed component to the basal particles and can thus produce granular agitation. A different basal boundary condition can be obtained by writing the heat flux $q_z(0)$ at the bed. $q_z(0)$ is equal to the balance between (1) the work done by shear stress, $\tau_{xz}(0)$, due to a basal slip at speed $u_{bed} = D\frac{\mathrm{d}u_x}{\mathrm{d}z}(0)$ (producing granular temperature) and (2) the dissipation term, $-D\Gamma(0)$, due to inelastic collisions integrated over the boundary layer (e.g. *Jenkins and Askari*, 1999; *Andreotti et al.*, 2013)

$$q_z(0) = D\frac{\mathrm{d}u_x}{\mathrm{d}z}(0)\tau_{xz}(0) - D\Gamma(0). \tag{S15}$$

After substituting expressions for q_z, $\frac{\mathrm{d}u_x}{\mathrm{d}z}$, τ_{xz} and Γ, Eq. (S15) simplifies to

$$\frac{\mathrm{d}S}{\mathrm{d}z}(0) = DAS(0) - \frac{5DB}{2}\overline{u}_x. \tag{S16}$$

Using the analytical solution of Eq. (S13) in Eq. (S16), and defining $A' = DA$, $B' = 5DB\overline{u}_x/2$, we obtain a second condition on c_1 and c_2,

$$A'(c_1 + c_2) + \sqrt{A}(c_2 - c_1) = f_3(h), \tag{S17}$$

where $f_3(h) = \frac{9\sqrt{\pi}BC}{16A^{7/4}}(A'f_1(h) + \sqrt{A}f_2(h)) - \frac{3BC}{2A}(\frac{3}{2}\sqrt{h} + A'h^{3/2}) + B'$, with

$$f_1(h) = \mathrm{erf}(A^{1/4}\sqrt{h})\exp(\sqrt{A}h) - \mathrm{erfi}(A^{1/4}\sqrt{h})\exp(-\sqrt{A}h) \tag{S18}$$

$$f_2(h) = \mathrm{erf}(A^{1/4}\sqrt{h})\exp(\sqrt{A}h) + \mathrm{erfi}(A^{1/4}\sqrt{h})\exp(-\sqrt{A}h). \tag{S19}$$

Finally, using both conditions (S14) and (S17), we obtain values of the constants

$$c_1 = \frac{f_3(h)}{A'(1 - \exp(2\sqrt{A}h)) - \sqrt{A}(1 + \exp(2\sqrt{A}h))}, \tag{S20}$$

and

$$c_2 = -\frac{f_3(h)\exp(2\sqrt{A}h)}{A'(1 - \exp(2\sqrt{A}h)) - \sqrt{A}(1 + \exp(2\sqrt{A}h))}. \tag{S21}$$

The exact solution for the average fluctuating speed $\delta u(z)_{kin}^{exact} = S(z)^{1/3}$ is plotted in Fig. S4 along with the approximate solution $\delta u_{kin} = \sqrt{T(z)}$, where $T(z)$ is given by Eq. (S10). The approximate solution with Eq. (S10) is close to the exact solution, especially for large values of the ratio $h/D \geq 10$. Since Eq. (S10) does not depend on the uncertain boundary conditions, we recommend the use of the approximated $\delta u(z)_{kin}$ for computation of the rate of particle impact and basal impulses per impact in the flow body and snout for thick debris flows in very smooth channels (for which Eq. (S11) dominates Eq. (S1)).

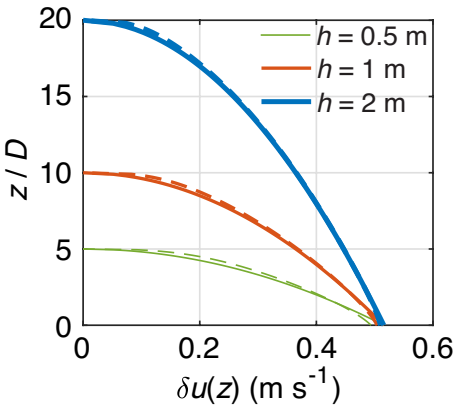

Figure S4: Average fluctuating speed $\delta u(z)_{kin}$ using the kinetic theory of granular gases obtained assuming $p = 3/2$ (Bagnold profile), for different h, with $\overline{u}_x = 10$ m s^{-1}, $D = 0.1$ m, $\phi = 0.6$, $e = 0.5$ and $\theta = 10°$. $z = 0$ corresponds to the location of the first particle above the bed. Solid lines denote the exact solution $\delta u(z)_{kin}^{exact} = S(z)^{1/3}$ with $S(z)$ given by Eq. (S13) whereas dashed lines denote approximation $\delta u(z)_{kin} = \sqrt{T(z)}$ using Eq. (S11) with $p = 3/2$. Results for all thicknesses have similar magnitudes because $\overline{u}_x$ is assumed to be the same (10 m s^{-1}) for all thicknesses. In reality, $\overline{u}_x$ is expected to increase with flow thickness.